

# Performance Analysis of Hybrid Excitation Flux Switching Permanent Magnet Motor for PHEV Application

Sid Ali Randi<sup>1,2</sup>

<sup>1</sup>VEDECOM, 23 bis allée des maronniers – 78000 Versailles - France, [sid-ali.randi@vedecom.fr](mailto:sid-ali.randi@vedecom.fr)

<sup>2</sup>RENAULT S.A, Technocentre Renault – I, avenue du golf – 78288 Guyancourt - France, [sid-ali.randi@renault.com](mailto:sid-ali.randi@renault.com)

---

## Summary

This paper presents the performance analysis of a Hybrid Excited Flux Switching Permanent Magnet machine designed for PHEV application. The working principle of the Flux Switching Machine with Hybrid Excitation is explained and the advantages of Hybrid Excitation are highlighted. The  $dq$  Park theory is used to model the machine by means of magnetization curves obtained from FEA analysis. Combination between the FEA results and analytical modelling allow to evaluate the whole performances of the machine in its torque-speed working plane. The optimal control strategy that allow to find the three currents for each working point in the torque-speed plane is obtained by optimization algorithm. The *fminimax* function in MATLAB® is used to minimize the losses within the Volt-Amp limits of the inverter. The approach used allow to map all the performances of the motor. In the final paper a particular attention is given to the induced voltage in the DC excitation winding. The torque ripple and power factor also can be an issue for this kinds of machines. The actual design exhibit a high level of cooper losses in max-power region and max-torque region, the maximum field excitation current is needed in these regions. A prototype of the machine is under construction and we except a complete presentation of the measured efficiency and motor parameters in future work.

---

*Keywords: Permanent Magnet Motor, PHEV (Plug In Hybrid Electric Vehicle), Finite Element Calculation, Efficiency, Power Factor (PF), Optimization.*

---

## 1 Introduction

In the last ten years, there is more and more interest on Flux Switching Permanent Magnet FSPM machines [1]. These machines are presented as permanent magnets PMs synchronous machines where the magnets are located on the stator. The rotor is similar of that one of Doubly Salient Switch Reluctance Machine. Putting the magnets in the stator is interesting from thermal point of view. In classical Interior Permanent Magnet machines IPM used for EV and HEV applications the PMs are located on the rotor and often associated with concentered winding in the stator, this may cause magnets over-heat and demagnetization. In FSPM machines the magnets are not far from the cooling source in case of water jacket cooling. For a given EV or HEV application when we want to replace IPM machine or EESM machine with

equivalent FSPM machine that fulfill the same requirements, the global cost must be considered, not only the cost of the machine itself but also efficiency cost. Replacing classical IPM machine with FSPM machine seems not be interesting because the magnets quantities engaged to fulfill torque and power requirement are more then what we need for the IPM machines [2]. To overcome this obstacle, the idea which consists to combine PMs and DC current Field Excitation Circuits DC-FECs is used. The advantages of both PMs and DC-FEC synchronous machines are then combined. These kind of FSPM machines are called Hybrid Excitation Flux Switching Permanent Magnet HEFSPM machines. As such HEFSPM machines have the potential to improve flux weakening performances, high power and torque density, variable flux capabilities.

In this paper we present the performance analysis of 12 slots – 10 teeth HEFSPM machine designed before for PHEV application [3]. After a brief description of operating principle of HEFSPM machine. The  $dq$  Park approach theory is used to establish the mathematical model of the machine. Direct axis d-axis flux  $\Phi_d$  and quadrature axis flux q-axis  $\Phi_q$  are considered as function of three currents, d-axis current  $I_d$  and q-axis current  $I_q$  and the Field Excitation DC current  $I_f$ . Finite Element Analysis FEA is used for flux mapping when the three currents  $I_d, I_q, I_f$  are varying within their limits. FEA analysis are also used to compute the different losses of the motor over the 3D-grid of  $I_d, I_q, I_f$ . Combination between FEA computation and analytical equations of the machine allow us to find all performances of the motor over the torque-speed plane. We are now building the prototype of the machine Fig.1(c). In the final paper we will present a comparison between FEA commutated efficiency and measurement efficiency. We want to do this comparison especially on some representative points for the WLTC cycle. The main goal for us, is to compare in terms of efficiency this HEFSPM machine with existing machines used for HEV applications.

## 2 Operating Principle of HFSPM

The cross-section of the 3-phases 12 slots-10 rotor teeth of HEFSPM machine is presented in Fig.1(a). The rotor is similar to that we can find in switch reluctance (SR) machine. In the stator of 12/10 – HEFSPM machine there is an elementary magnetic circuit (EMC) repeated 12 times. This EMC is presented in Fig.1(b).

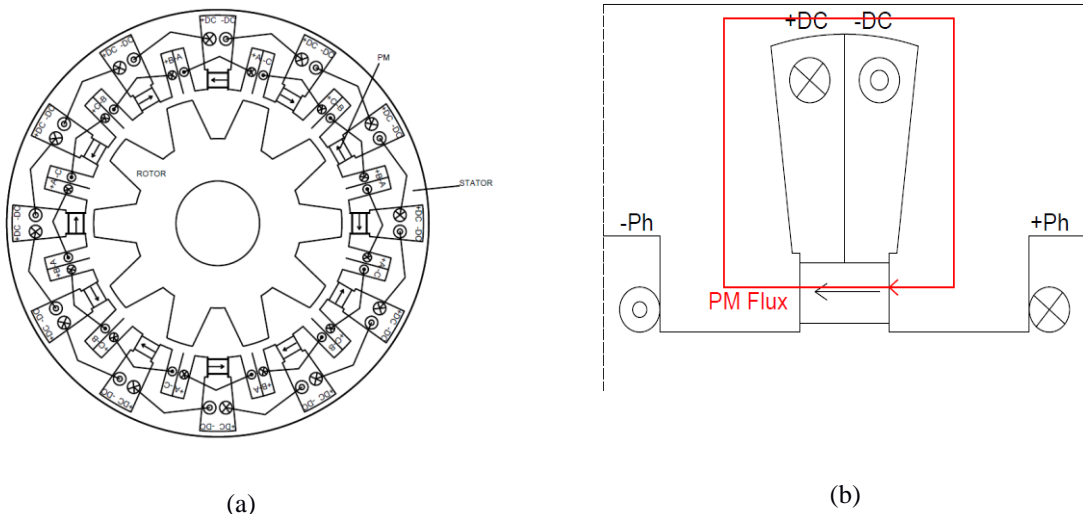


Figure 1: (a) Cross-section of the 3-phases 12/10 HEFSPM machine – (b) Elementary Magnetic Circuit

In each EMC, there is one PM circumferentially magnetized, plus and minus conductors for a given phase (A, B or C), +DC and -DC conductors located in the slot above the PM. The magnets of two adjacent EMCs are magnetized in opposite directions. Each phase is composed by 4 EMCs spaced by  $90^\circ$  mechanical. The coils for phases and excitations are connected in series.

Fig. 2 illustrate the operating principle of this HEFSPM machine for three different positions of the rotor. If the excitation current is equal to zero the PM flux is short-circuited behind the back iron of the DC slot Fig.1(b). Putting DC current lead to the saturation of the back iron region located behind the DC current

slots, this force the PMs and field excitation fluxes to pass through the airgap. These fluxes are commutated by the rotor teeth. In Fig.2 (a), theses fluxes goes from the stator to rotor tooth Th2 and come back to the stator from the rotor tooth Th3. Meanwhile, in Fig. 2(b), when the rotor moves to left side approximately half electric period, both fluxes from stator flow to rotor tooth Th1 and come back to the stator through rotor tooth Th2 and the airgap. It is clear that the stator fluxes generated by PMs and FE windings switches their polarities through rotor tooth Th1 as receiving flux, while rotor tooth Th2 bringing flux back to stator. Fig.2(c) represent the same position as Fig.2(a) where the rotor teeth Th2,Th3 are replaced by Th1,Th2 respectively. During a complete electric cycle of  $36^\circ$  mechanical (the number of pole pair  $p = 10$  is equal of the number of rotor teeth), the flux seen by the phase “A” is assumed as sinusoidal. Hence the induced back-emf in the phase winding is also sinusoidal. In Fig.2 (d) we represent the back-emf and its harmonics components Fig.2 (e) at 1000 rpm of the real machine computed by mean of FEA. The harmonics components show that the sinusoidal hypothesis is valid. So the machine is seen as synchronous machine and the Park approach is used to describe the electromagnetic behavior of the machine. It is what we present in the next section.

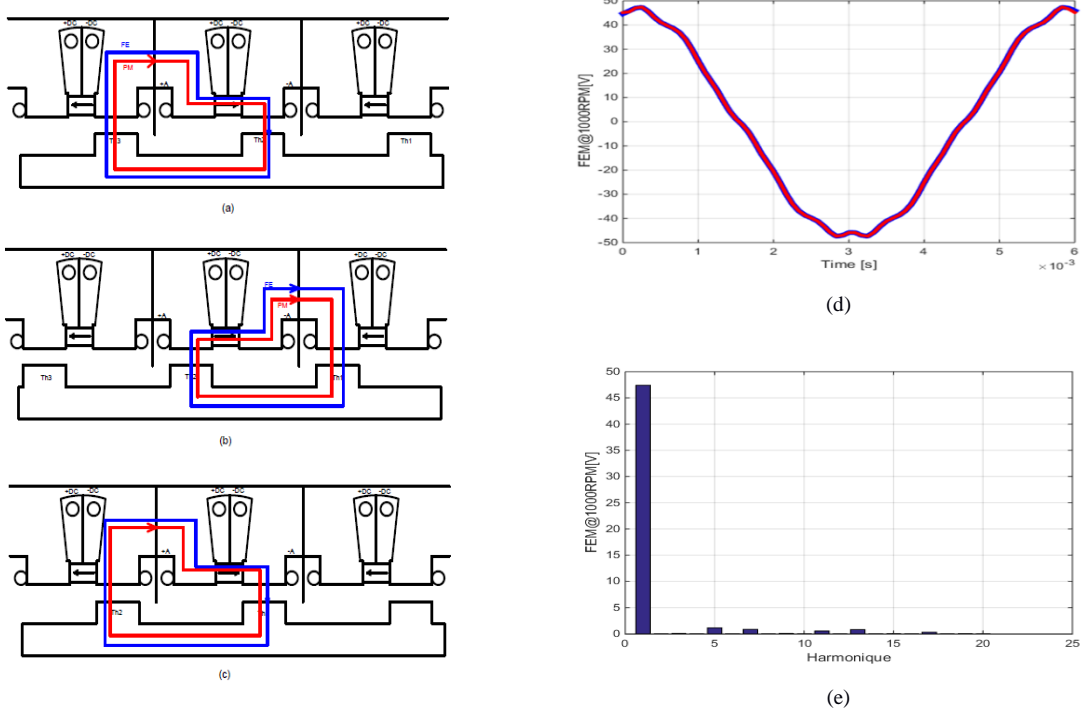


Figure 2 : (a) Principle of operation of 12-10 the machine – (b) back-emf @ 1000rpm – (c) Harmonics of back-emf

### 3 Mathematical Model and FEA Analysis

#### 3.1 Flux mapping of HEFSPM

The  $dq$  theory is widely used in the modelling and analysis of synchronous machines because it allow a great simplification of the equations. It is mathematical transformation based on the observation of the different quantities on a new reference frame. Using this transformation is based on some assumptions that should be fulfilled in order to get reliable models: The windings should be sine-distributed and magnetic circuit is assumed not saturated. In first approach it is not obvious to use this transformation for HEFSPM machines. There is concentrated winding. Authors in paper [4] demonstrate that Park transformation can be extended to machine with concentrated winding. Works presented in [5], shows that the  $dq$  model is credible to predict the performance of HEFSPM motor over its operating range in the torque speed plane.

In our case we consider the magnetization curves :i.e., the relationship between the fluxes in the d-axis and q-axis  $\Phi_d$ ,  $\Phi_q$ , and the three currents: d-axis  $I_d$ , q-axis  $I_q$  and field excitation current  $I_f$ :

$$\Phi_d = \Phi_d(I_d, I_q, I_f); \Phi_q = \Phi_q(I_d, I_q, I_f) \quad (1)$$

Commercial FEA software MAXWELL-2D® is used to map the above magnetizing curves within the limits of the 3 currents:

$$I_d \in [-400, 400] \text{Amps}; I_q \in [-400, 400] \text{Amps}; I_f \in [-50, 50] \text{Amps} \quad (2)$$

The grid used for this mapping is 9 points for  $I_d$ , 9 points for  $I_q$ , and 5 points for  $I_f$ . This leads to 405 2D-FEA computations made on the whole machine. The computations were made for 2 electrical cycles, the time discretization is  $0.5^\circ$  electrical, and the speed is 1000 rpm. 2 cycles and  $0.5^\circ$  are taken, because we compute not only the fluxes but also all the other motor performances for the chosen grid: Torque, Fluxes, Iron Losses, Magnet Losses, Induced voltage in the field excitation winding ...etc. Fig.3(a) and Fig.3(b) present the q-axis flux and d-axis flux as function of the currents  $I_d$  and  $I_q$  for excitation field current  $I_f=50$  Amps.

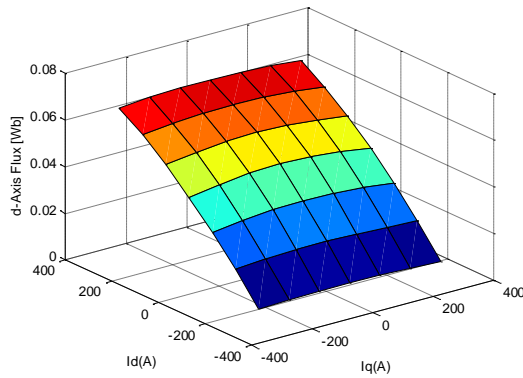


Fig.3(a): FEA- d-Axis Flux

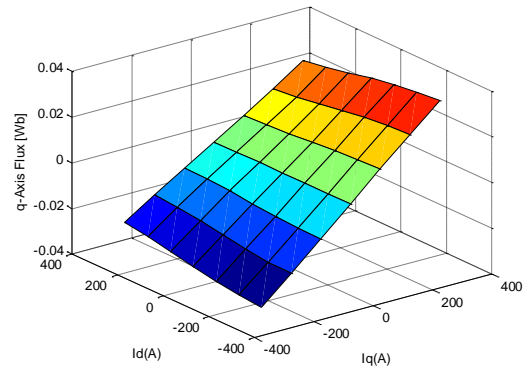


Fig.3(b): FEA- q-Axis Flux

The total d- and q- axis flux-linkage equations satisfy:

$$\begin{cases} \Phi_d = \Phi_v + L_d I_d \\ \Phi_d = L_q I_q \end{cases} \quad (3)$$

Where  $L_d$  and  $L_q$  are the d-axis and q-axis inductances, they are presented in the  $I_d$ - $I_q$  plane in the Fig.4(a) and Fig.4(b) respectively, for excitation field current  $I_f=50$  A.

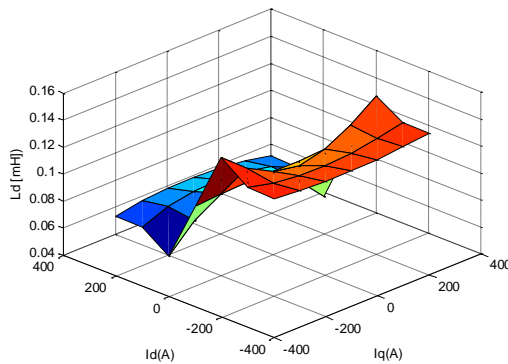


Fig.4(a): d-Axis Inductance for  $I_f=50$ A

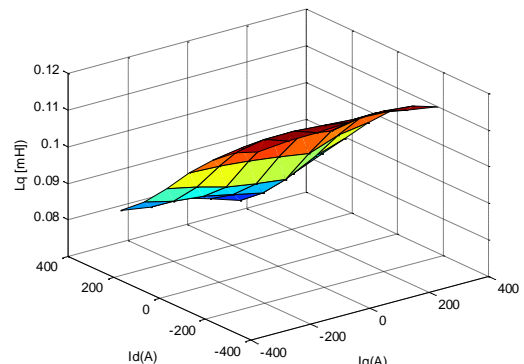


Fig.4(b): q-Axis Inductance for  $I_f=50$ A

An important value is the flux-linkage  $\Phi_v$ , which is the maximum value of the flux due to PMs and Field Excitation Current  $I_f$ . It was computed by FEA for different excitation currents and different combinations of  $I_d, I_q$ . The value for  $I_f = 50$  Amps and  $N_{exe} = 50$  turns ( $N_{exe}$  : Number of excitation turns per coil) was  $\Phi_v = 45.34$  mWb. The machine exhibit the behaviour of Surface Mounted Permanent Magnet SPM motor, the saliency ratio is around unity as shown in the Fig.5

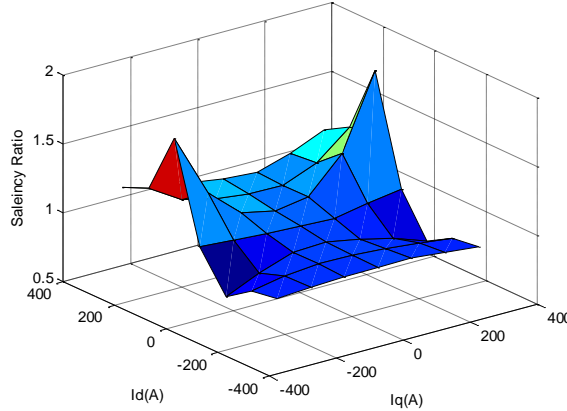


Fig.5: Saliency Ratio

The  $d$ - and  $q$ - axes voltage equations are obtained below:

$$\begin{cases} V_d = \frac{d\Phi_d}{dt} - \omega_e \Phi_q + R_s I_d \\ V_q = \frac{d\Phi_q}{dt} + \omega_e \Phi_d + R_s I_q \end{cases} \quad (4)$$

Where the inverter frequency  $\omega_e$  is related to the rotor mechanical speed  $\omega_m$  and pole pair number  $P$  as follow :

$$\omega_e = P \omega_m \quad (5)$$

The electromagnetic torque is given by the following equation:

$$T_{em} = \frac{3}{2} P [\phi_v I_q + (L_d - L_q) I_d I_q] \quad (6)$$

### 3.2 Losses Computation and Optimal Control Strategy

Magnetization curves computed by FEA at 1000 rpm as explained in the previous section. In the same time the different losses normalized by the speed are computed for each triplet  $(I_d, I_q, I_f)$ . We take the assumption that iron hysteresis losses are proportional to the electrical frequency  $\omega_e$ . Iron and magnets eddy current losses are proportional to the square of the electrical frequency  $\omega_e$ . The mechanical losses can be expressed according to the following equation :

$$P_{mech} = \alpha \omega_m + \beta \omega_m^2 + \gamma \omega_m^3 \quad (7)$$

Where the coefficients  $\alpha, \beta, \gamma$  are identified from experimental measurement. Joule losses in armature coils and in Field Excitation coils are calculated at 100°C from the measured values of armature coils resistance  $R_s$  and Field Excitation coils resistance  $R_f$

For a given DC voltage, within the Volt-Amp limits of the inverter [7], and for each operating point of the torque-speed plane we have to find the three currents  $I_{dx}, I_{qz}, I_{fx}$  that allow the total Joule losses minimization. The *fminimax* function in MATLAB® is used for this purpose. Fig.6(a) and Fig.6(b) present the mapping of  $I_d$  and  $I_q$  currents for DC voltage equal to 400 V and Maximum RMS Currents of the Inverter lower than 262 Arms. Different control strategy can be adopted, either minimization of total Joule losses or minimization of total machine losses. For our case, we adopt the Maximum torque per Ampere strategy i.e Joule losses minimization. Before base speed, the control strategy confirm that essentially q-Axis current produce the torque while d-axis current is kept near zero by the algorithm. From Fig.6 (a & c) q-Axis current and FE excitation current contribute to torque in the same proportion. Above base speed one can see from Fig.6(d) phase voltage saturation, the whole available voltage is used.

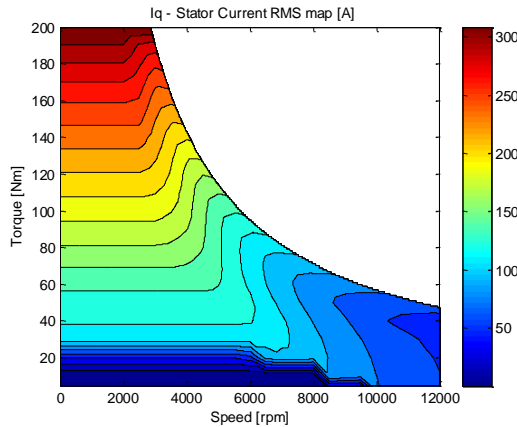


Fig.6(a): Optimal q-Axis current -  $V_{dc}=400V$

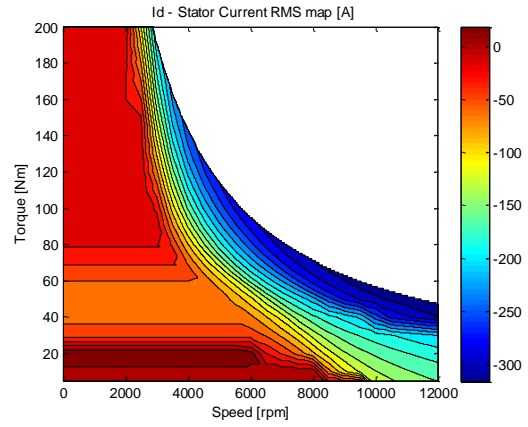


Fig.6(b): Optimal d-Axis current -  $V_{dc} = 400V$

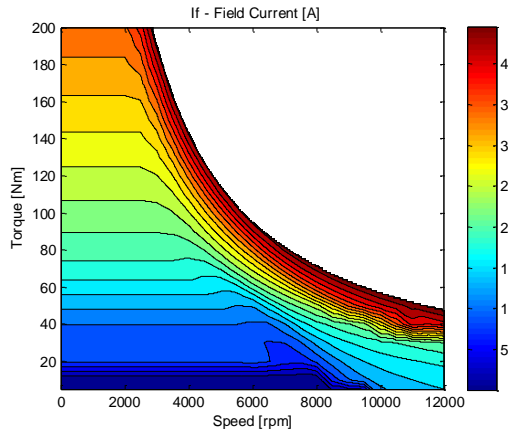


Fig.6(c): Optimal Excitation Current  $I_f$

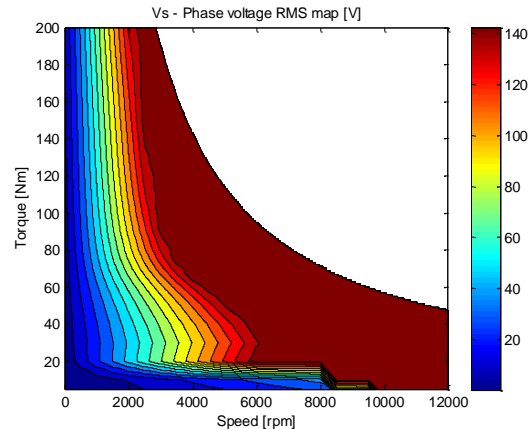


Fig.6(d): RMS Value of phase Voltage  $= 0.9 \frac{V_{dc}}{\sqrt{6}}$

### 3.3 Results Analysis and discussion

From Fig.7(a) one can see that Power Factor – PF is low in the most operating working points of WLTP cycle i.e. between 0 – 50 Nm and 0 – 5000 RPM. Nevertheless, the PF is good above base speed. There is another issue related to HEFSPM, it is the induced voltage in the Field Excitation coils. In Fig.7(b), it can be seen that the RMS value of the induced voltage in the FE coils can be greater than 450V. We have in fact alternative waveform with average value equal zero. But the DC chopper for the FE supply current is designed to take into account this problem.

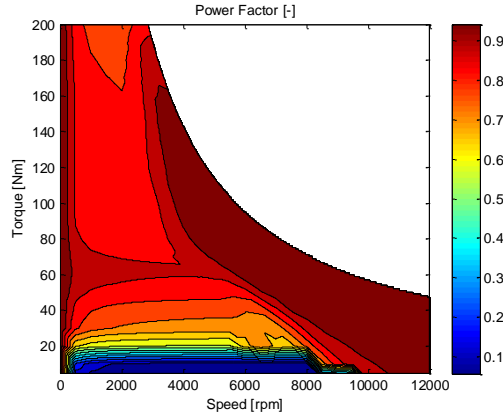


Fig.7(a): Power Factor -  $V_{dc}=400V$

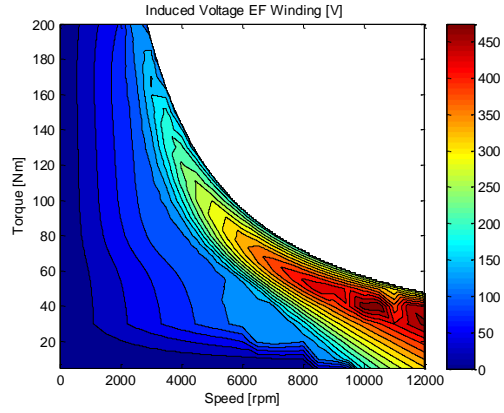


Fig.7(b): Induced Voltage in Excitation Coils

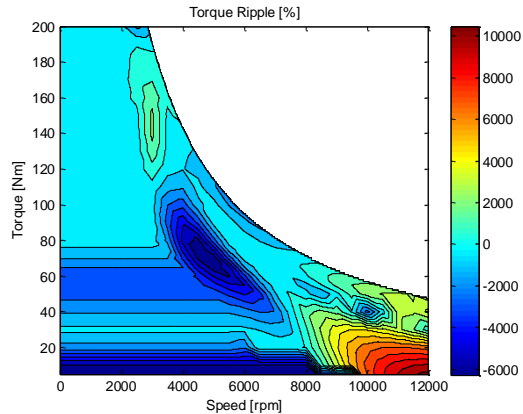


Fig.7(c): Torque Ripple in [%]

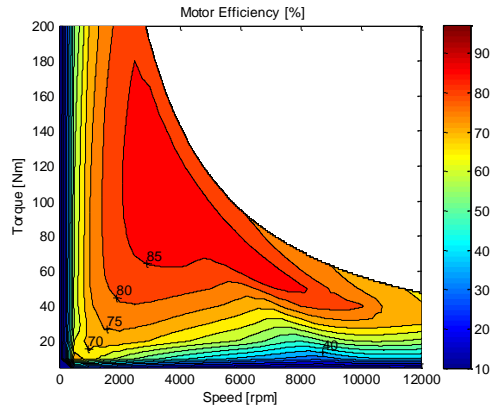


Fig.7(d): Motor Efficiency

The torque ripple in HEFSPM can be also an issue, from Fig.7(c), one can see that depending on the region of the torque-speed plane, the torque ripple can be important. The testing motor will confirm or not this high levels of torque ripple. In Fig.7(d) is presented the motor efficiency map. It can be seen that in the working points for hybrid application, the efficiency is few points lower than the values expected for equivalent IPM motor installed on the TOYOTA PRIUS 2010 [6]. For prototype motor, we expect worst results than those obtained by FEA computation. Indeed, for FEA models the AC cooper losses are not yet taken into account. Before going on huge computation of AC losses we prefer measure the data from experimental motor.

## 4 Design Constraints Target Specifications and Prototype

### 4.1 Typeface and Sizes

To validate the results obtained by FEA analysis we are building now a prototype of the HEPMFS machine. Table I presents the design restrictions of the machine for the considered PHEV application. The peak power must be greater the 60 kW (18s) and the continuous power must be 21kW. As motor size constraints, the stator outer diameter is set to 260 mm, and the active motor length is 100m. The airgap length is 0.8mm and the total magnet weight must be lower than 700g. The electrical restriction related to the inverter are set to 262Arms per phase and 50 A for field excitation current. As thermal restrictions, our cooling is a water jacket cooling system as presented in Fig.8(b). As target specifications, the maximum torque must be greater than 200 Nm and the maximum speed is 12000 rpm. The material used for permanent magnet is N42SH and the electrical steel material used for stator and rotor lamination is M330-35 made by Arcelor.

Table I: HEFSPM Design Restrictions

Items	Value
Maximum DC-bus voltage [V]	400
Maximum current inverter [ $A_{rms}$ ]	262
Maximum current density in armature [ $A_{rms}/mm^2$ ]	35
Maximum current density in excitation coils [ $A/mm^2$ ]	35
Stator outer diameter [mm]	260
Motor stack length [mm]	110
Airgap length [mm]	0.8
Maximum PM weight [g]	700
Maximum speed [rpm]	12000
Maximum torque [Nm]	200
Peak power [kW]	60
Time @ peak power [s]	18
Rated power [kW]	21
Maximum temperature in wires [ $^{\circ}C$ ]	180
Material used for permanent magnets	N42SH
Material used for laminations	M330-35

The major machine dimensions are the results of multi-objective optimization using genetic algorithm under the specification constraints presented in the table I [3]. The maximum torque point (200Nm, 2865 rpm, 60 kW) and high speed point (47.7 Nm, 12000 rpm, 60 kW) must be achieved.

### 4.2 Prototype building

The motor dimensions and major electrical parameters of the prototype are presented in table II. Fig (8) shows photographs of stator assembly, rotor, shaft and housing. The magnet dimensions are 6.56x9.99x55mm<sup>3</sup>, there two magnet segment in the axial direction. The total magnet weight is 648 g and the total machine weight is 33 kg. The expected torque density of the machine is 6.51 Nm/kg and the estimated cost in serial production for automotive applications is estimated around 300 € in 2020.

Table II: Test Motor Specifications

Items	Value
Outer Stator Diameter [mm]	260
Active Axial Length [mm]	110
Outer Rotor Diameter [mm]	194.7
Shaft Diameter [mm]	50
Coil-end length (connection) [mm]	50
Coil-end length (non-connection) [mm]	30
Number of turns / coil – Armature winding x Parallel wires( $\Phi$ mm)	5x6(1.25)
Filling factor – Armature winding [%]	55
Resistance Armature winding @ 20°C - $R_s$ [mΩ]	22.35
Type of connection Armature winding	3 Ph – Series - Y
Number of turns / coil – Excitation Field winding x Parallel wires( $\Phi$ mm)	50x4(0.75)
Filling factor – Excitation Field winding[%]	48
Resistance Excitation Field winding @ 20°C - $R_f$ [Ω]	2.4
Type of connection Excitation Field winding	DC – Series

The machine is now under assembly, the comparison between FEA results and measured efficiencies will be presented in future works. In order to get a good resolution, a specific 10-pole resolver made by Tamagawa is used. This specific order lead to a delay in the motor assembly and testing.



Fig.8(a): Wounded stator of HEFSPM



Fig.8(b): Housing, Rotor and Shaft of 1<sup>st</sup> prototype of HEFSPM

## 5 Conclusions

In this paper, design, FEA studies and performance analysis of 12 slot- 10 pole HESFPM for PHEV traction drive application have been presented. The machine is of synchronous type, even if the flux density distribution in the airgap is far from sinusoidal waveform. The d-q Park Theory has been used to establish the mathematical model. The d-q fluxes computed by means of FEA analysis shows that from electromagnetic point of view, the machine exhibit the behaviour of SPM-Permanent magnet machine with saliency ration near unity.

An optimization algorithm has been used, to find the optimal currents that allow losses minimization, for each point in the torque-speed plane. Losses model based on 2D-FEA has been used to map the efficiency of the motor. It has been found that Joule losses are important in the torque region, and iron losses are dominant in the high speed region. Further optimization works must be done in the future in order to reduce the FE

coils resistance. For iron losses reduction the next prototype must be built with thinner steel. FEA results shows that all the target performances of the PHEV application have been achieved. To confirm the FEA results a prototype have been built all pieces received and assembly works of the first prototype is on-going now. HEFSPM seems interesting from torque and power densities point of view. The low cost of engaged material and the manufacturing process place this kind of machine as a serious candidate for automotive applications.

## References

- [1] E. Sulaiman, S.N.U. Zakaria, T. Kosaka *Parameter Sensitivity Study for Optimization of Single Phase E-Core Hybrid Excitation Flux Switching Machine*, IEEE International Conference on Mechatronics (ICM). (2015).
- [2] R. Cao, C. Mi and M. Cheng *Quantitative Comparison of flux-switching permanent-magnet motors with interior permanent magnet motor for EV, HEV, and PHEV Applications*, IEEE Transactions on Magnetics, vol.48, no. 8, pp.2374-2384, Aug 2012.
- [3] N. Faltakh, S. Hlioui, M.Gabsi, R. Benlamine, F. Vangraefschep *Design of a Low Magnet Mass Hybrid Excited Flux Switching Machine for a PHEV Application*, International Conference on Electrical Machines, Drives and Power Systems (ELMA). (2017).
- [4] F. Meier, J. Soulard *dq Theory Applied to a Permanent Magnet Synchronous Machine with Concentrated Windings*, 4<sup>th</sup> IET Conference on Power Electronics, Machines and Drives. (2008).
- [5] A. Zulu, B.C. Mecrow, M. Armstrong *Prediction of Performance of a Wound-field Segmented-Rotor Flux-Switching Synchronous Motor Using a dq-Equivalent Model*, International Conference on Electrical Machines (ICEM). (2010).
- [6] H. Nakane, T. Kosaka, N. Matsui *Design Studies on Hybrid Excitation Flux Switching Motor with High Power and Torque Densities for HEV Applications*, 2015 IEEE International Electric Machines & Drives Conference (IEMDC). (2015).
- [7] S.A.Randi, S. Astier *Parameters of Salient Pole Synchronous Motor Drives with Two-Part Rotor to Achieve a Given Constant Power Speed Range*, 2001 IEEE 32<sup>nd</sup> Annual Power Electronics Specialists Conference (PESC). (2001).

## Authors



Sid Ali Randi received the Engineering degree in electrical engineering from Ecole Nationale Polytechnique, Algiers, 1995, and Ph.D. degree from Institut National Polytechnique de Toulouse, Toulouse, France, in 2003. He has more than 15 years' experience in the design and simulation of electrical machines and electrical drives for different industrial applications, in particular, axial and radial flux permanent magnet motors for electric mobility. He is currently a Research and Development Engineer in Electric Machines and Drives with the Simulation Department, Renault Technocenter, Guyancourt, France. He is also working as R&D Engineer at VEDECOM Institute. He is mainly working now on the design of innovative eMachines for EV and HEV applications.